Development of a Power and Voltage Control Scheme for Multi-Port Solid State Transformers

Mehdy Khayamy[†], Adel Nasiri[†], and Necmi Altin[†§]

[†]College of Engineering and Applied Science , University of Wisconsin-Milwaukee, 3200 N Cramer St, Milwaukee, WI, USA 5321 , nasiri@uwm.edu, Tel:(414) 229-4955

[§]Department of Electrical and Electronic Engineering, Faculty of Technology, Gazi University, Ankara, Turkey

***Abstract*—Solid State Transformers (SSTs) are being considered as a replacement to the classic transformers especially for renewable energy and energy storage systems mainly due to their much smaller size and controllability and regulation over the transferred power. Multi-Port SSTs share one high frequency core for the isolation between several devices and hence are even more compact and efficient but the system is complex and the control of such a system is a challenge. This paper considers a four-port, MPSST connected to a renewable source, battery, load, and the grid and discusses various scenarios and operating points. It is shown that several factors including the ratio of the renewable power to the load, battery SOC status and role of the battery in the system change the desired power flow in the system and there are several control structure needed for each mode of operation. These modes of operation and the boundary between them are recognized and eventually a MIMO control scheme is suggested that includes several switches to changes the structure of the controller to adjust the controller structure to the operating condition. Eventually, input-output linearization technique has been adopted to the system to linearize the model and achieve a better control performance.**

***Index Terms*—Input-Output linearization; MIMO control system; multi-port; solid state transformer.**

I. Introduction

A solid-state transformer (SST) have been an important candidate to replace the conventional low-frequency transformer (LFT) due to their reduced size, lower weight and enhanced functionalities. The initial studies on SSTs have been presented in 1970s [1], and they have been investigated for high power density systems such as traction and power distribution system applications [2]–[4]. Increasing renewable penetration to the grid and rising smart grid concept have made them popular for low to medium voltage level applications with their unique features such as VAR compensation, voltage regulation, fault isolation, and DC connectivity [5], [6]. The main difference between the SST and the conventional LFT is the medium- to high-frequency isolation. Although this medium- to high-frequency isolation requires additional power electronics converters, it still provides significant improvement in size and weight.

Since both input and output of the SST are connected to power electronics converters and controlled continuously, multi-port SSTs (MPSSTs) have been presented to integrate more than one energy sources such as distributed generation (DG) and/or energy storage system into load or utility grid [7]–[9]. Proper design of the turn ratios of the MPSST provides interconnection of different kind sources with different voltage levels. In [10], a MPSST has been proposed and controlled as an inter-grid power flow controller. In this study the MPSST with three-port is used to interconnect the renewable, battery and utility grid. A three-port SST employing two different transformers has been also proposed. In this system, a three-leg inverter is employed to provide parallel connection of the two secondary windings. It is reported that, one of the source can be disconnected form the system easily, and the circulating current is reduced. While one of the input port is responsible with output voltage control, the other one provides balanced power distribution between the windings. However, it requires higher number of switches and two separate transformers [11]. In [12], a three-port MPSST has been proposed for a fuel cell-storage hybrid energy system. Three ports are connected to the fuel cell, the energy storage (battery or super-capacitor) and the load. However, for the second storage device, second three-port transformer is used and controlling these two three-port transformers is proposed instead of single four-port transformer and controller design [12].

In [7], a MPSST with four ports to interconnect the PV system, battery energy storage unit, the load and the utility grid have been presented. An average model is presented for the converter circuits. Single-input single-output techniques with different bandwidths have been used for the control design [7]. The phase shift modulation method is commonly used in dual-active bridge converters and MPSST applications. However, the converter should be properly designed to obtain zero-voltage switching (ZVS) for entire operation range. In addition, the circulating current is high with this method [13]. Triangular current modulation strategy which uses the duty cycle to control the power transferred among the bridges is also applied to the four-port MPSST [13], [14]. The zero-current switching for converter switches and lower circulating current can be achieved with this modulation strategy. However, because of the triangle wave of the current, the root-mean-square (rms) value of the current on switches and transformer can be higher which may lead higher conduction losses [13].

A MPSST with n-port requires n converter circuits. The power flow between the ports of the MPSST can be controlled with the phase-shift angle between the gate signals applied to each converter. Although this increases the control degree-of-freedom, it also increases the control system complexity in case of higher number of ports.

978-1-5386-5982-3/18/$31.00 ©2018 IEEE

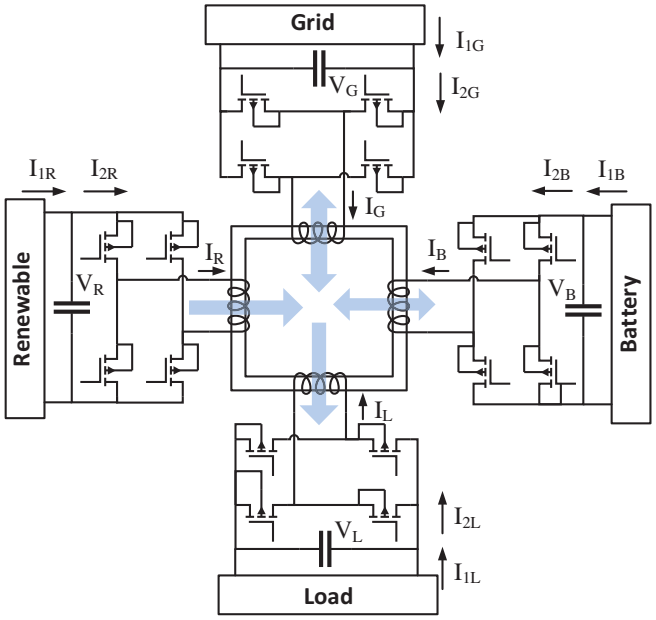

Fig. 1. A four-port MPSST, topology and power flows.

In this study, a four-port SST which is connected to a renewable energy source, battery based energy storage, load and the grid is proposed, as shown in Fig. 1. The operation modes of the proposed MPSST has been analyzed related to state of charge (SoC) of battery, power level of renewable energy source and the load demand. The multi-input-multi-output (MIMO) control scheme is presented to define the operation modes and to control the whole system. Performance of the proposed control system is validated through the MATLAB/Simulink simulation results.

II. Modes of Operation

A four port MPSST is considered in this paper. Ports are connected to the grid (G), renewable (R), Battery (B), and the load (L). Fig. 1 shows the power flow in such a MPSST. While the renewable and load are one directional, battery and grid can transfer bidirectional power. Four conditions can happen based on the renewable power in compare to the load power as shown in Fig. 2. Condition *a* is when the renewable power is much higher than the load, the load demands much higher power than renewable can provide in *d* and *b,c* fall in between.

Three scenarios of operation have been considered in this paper. In the first scenario, the system is connected to the grid but the battery is only available for UPS like reserve and needs to be charged but not used as it is shown in Fig. 3. The direction of the power depends on the relative power of the renewable and the load ,conditions, as well as the battery SOC.

The battery can be charged and discharged freely in the second scenario, Fig. 4, and the third scenario describes an autonomous system, Fig. 5. The desired power flow is shown in each scenario based on the conditions and SOC of the battery in Figs. 3-5. Also, the control strategy for each port is summarized with orange font color in these figures.

The power transfer is being realized by phase shifting the square wave output of H-bridge converters connected to each port. The power transfer equation for a two port SST, is shown in (1) where φ is the phase shift between ac voltages [15].

$$P = \frac{nV_1V_2}{2Lf\pi^2}\varphi(\pi - \varphi) \tag{1}$$

The angle reference is considered to be the load converter and all of the other phase shifts are compared to the load converter. The load port only receives power, therefore the angle of this port is considered the maximum of $\varphi_L = \pi/2$. Fig. 6 summarizes the phase shift control policy on the of each port to achieve the required power flow. The table makes it clear that the load voltage needs to regulated at any time by either of the renewable, φ_R, battery, φ_B, or the grid, φ_G.

In scenario 1 and 2, regardless of conditions and SOC, renewable converter operates at maximum power point tracking (MPPT) because even if there is excessive power, it can be injected to the grid. For scenario 3 which is stand alone, if the renewable is generating more power than the load and battery maximum charge current, the control system of the renewable should change to the load regulation.

The battery converter either charges the battery at the maximum charge current, maximum discharge current, zero battery current or the load voltage regulation. The grid converter is either regulates the load voltage or regulates zero power at the grid port depends.

III. MPSST Model State Space Representation

State variables are capacitor voltages and transformer leakage inductance current. The assumption has been made that the magnetizing current is much smaller than the rest of the currents and the core does not saturate. Since all of the four converters are identical, the equations are written for one of them with subscript of x which can be R, B, G, or L. The top and bottom switches are complimentary and hence only top switches are mentioned here. S_{apx} and S_{bpx} are top switches of the first and second leg of any of the converters. To simply equations, the modulation index M_x is used as the difference between switching functions (2). DC link voltage equation is (4). C is the DC link capacitor.

$$S_{apx} - S_{bpx} = 2S_{apx} - 1 = M_x \tag{2}$$

$$\frac{d}{dt}V_x = \frac{1}{C}\left(I_{1x} - I_{2x}\right) \tag{3}$$

$$\frac{d}{dt}V_x = \frac{1}{C}\left(I_{1x} - M_xI_x\right) \tag{4}$$

To find the transformer current equations, KCL needs to be solved at the middle virtual node, V_o, of the transformer. The current on branch x is described by (5). r and L_l are winding resistance and leakage inductances respectively.

$$\frac{d}{dt}I_x = \frac{1}{L_l}\left(M_x\frac{V_x}{2} - V_o - rI_x\right) \tag{5}$$

Four transformer currents cancel out each other. By adding all four currents, V_o can be found as (7). (5) can be rewritten as

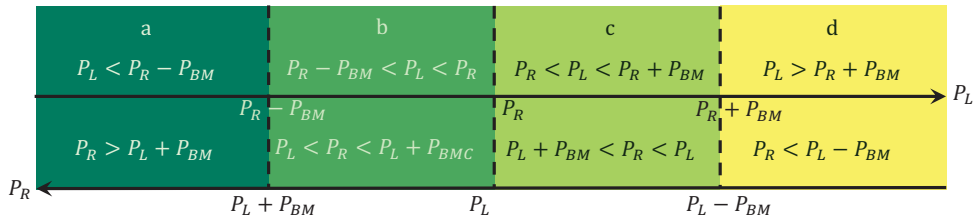

Fig. 2. The four possible conditions that describe possible relation between the renewable and load powers.

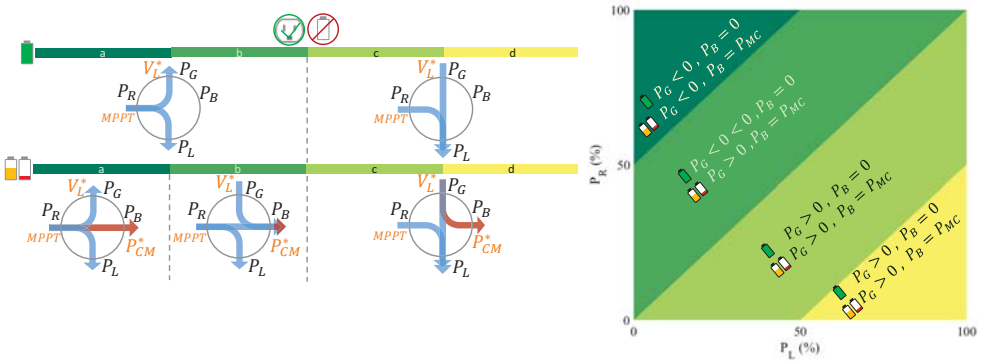

Fig. 3. Scenario 1, grid is available and the battery should be charged but not used.

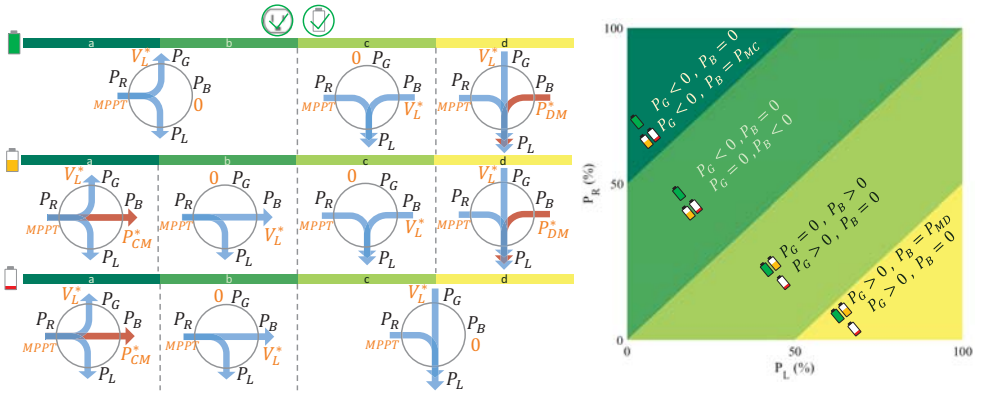

Fig. 4. Scenario 2, grid is available and the battery can be charged or discharged.

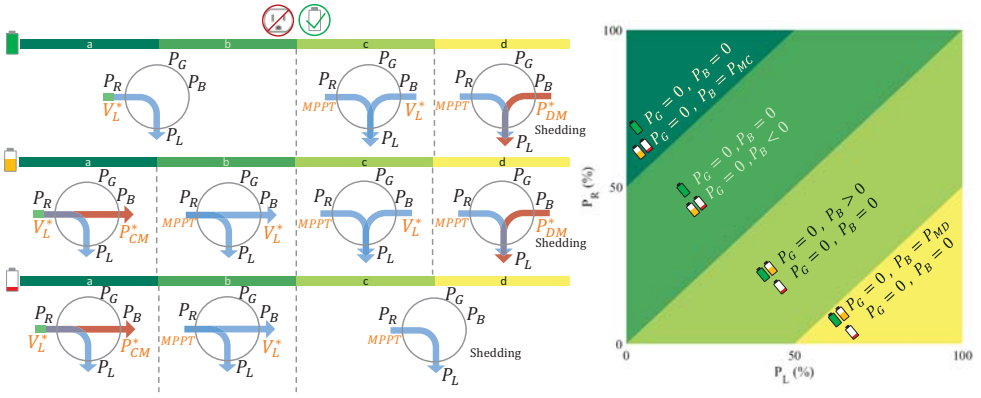

Fig. 5. Scenario 3, grid is not available.

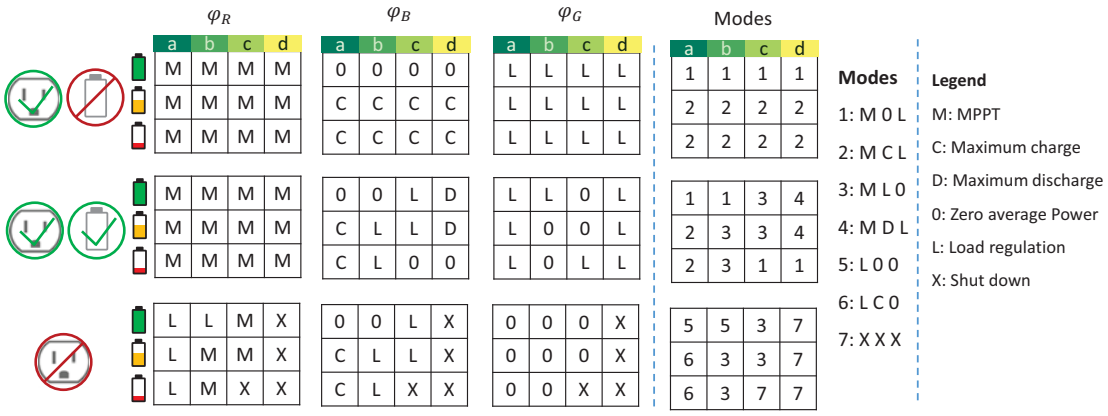

Fig. 6. Summarized control principal for each converter and all of the possible modes of operation.

(8).

$$0 = \frac{1}{L_l}\left(\sum M_i \frac{V_i}{2} - 4V_o\right) \tag{6}$$

$$V_o = \frac{1}{4}\sum M_i \frac{V_i}{2} \tag{7}$$

$$\frac{d}{dt}I_x = \frac{1}{L_l}\left(M_x \frac{V_x}{2} - \frac{1}{4}\sum M_i \frac{V_i}{2} - rI_x\right) \tag{8}$$

State space representation of the system described in Fig. 1 is shows in (18) which has the general form of (17). It is assumed the inverters generate square waveforms with the maximum duty cycle.

$$\frac{d}{dt}V_R = \frac{1}{C}\left(I_{1R} - M_R I_R\right) \tag{9}$$

$$\frac{d}{dt}V_B = \frac{1}{C}\left(I_{1B} - M_B I_B\right) \tag{10}$$

$$\frac{d}{dt}V_G = \frac{1}{C}\left(I_{1G} - M_G I_G\right) \tag{11}$$

$$\frac{d}{dt}V_L = \frac{1}{C}\left(I_{1L} - M_L I_L\right) \tag{12}$$

$$\frac{d}{dt}I_R = \frac{1}{8L_l}\left(4M_R V_R - (M_B V_B + M_L V_L + M_G V_G) - 8rI_R\right) \tag{13}$$

$$\frac{d}{dt}I_B = \frac{1}{8L_l}\left(4M_B V_B - (M_R V_R + M_L V_L + M_G V_G) - 8rI_B\right) \tag{14}$$

$$\frac{d}{dt}I_G = \frac{1}{8L_l}\left(4M_G V_G - (M_R V_R + M_B V_B + M_L V_L) - 8rI_G\right) \tag{15}$$

$$\frac{d}{dt}I_L = \frac{1}{8L_l}\left(4M_L V_L - (M_R V_R + M_B V_B + M_G V_G) - 8rI_L\right) \tag{16}$$

$$\frac{d}{dt}X = f + u_1 g_1 + u_2 g_2 + \cdots + u_m g_m \tag{17}$$

$$\frac{d}{dt}\begin{pmatrix} I_R \\ I_B \\ I_G \\ I_L \end{pmatrix} = \frac{r}{L_l}\begin{pmatrix} I_R \\ I_B \\ I_G \\ I_L \end{pmatrix} + \frac{M_R V_R}{8L_l}\begin{pmatrix} 3 \\ -1 \\ -1 \\ -1 \end{pmatrix} + \frac{M_B V_B}{8L_l}\begin{pmatrix} -1 \\ 3 \\ -1 \\ -1 \end{pmatrix} + \frac{M_G V_G}{8L_l}\begin{pmatrix} -1 \\ -1 \\ 3 \\ -1 \end{pmatrix} + \frac{M_L V_L}{8L_l}\begin{pmatrix} -1 \\ -1 \\ -1 \\ 3 \end{pmatrix} \tag{18}$$

IV. Applying Input-Output Linearization Technique

The four transformer currents are linearly dependent as one of them is the negative summation of the others (19). For the purpose of the control system the angle of the voltage on the load converter is considered as the reference angle for other the phase shift of other converters. The phase shift of the load converter is a constant value at 45° which is the middle of the $0 - 90^\circ$ range. The load current is eliminated in the state space representation of (18) to arrive at (20).

$$I_L = -(I_R + I_B + I_G) \tag{19}$$

$$\frac{d}{dt}\begin{pmatrix} I_R \\ I_B \\ I_G \end{pmatrix} = \frac{1}{L_l}\begin{pmatrix} rI_R - 1/8 M_L V_L \\ rI_B - 1/8 M_L V_L \\ rI_G - 1/8 M_L V_L \end{pmatrix} + \frac{M_R V_R}{8L_l}\begin{pmatrix} 3 \\ -1 \\ -1 \end{pmatrix} + \frac{M_B V_B}{8L_l}\begin{pmatrix} -1 \\ 3 \\ -1 \end{pmatrix} + \frac{M_G V_G}{8L_l}\begin{pmatrix} -1 \\ -1 \\ 3 \end{pmatrix} \tag{20}$$

Like most of the power electronic state space model, MPSST is nonlinear as well because it has input multiplied by state variables. Input-Output linearization has applied to the system to linearize it. Equation set of (20) is already in general from of (17). The relative order of all the state variables is 1 which simplifies the system. Applying input-output linearization to the system, the general form of matrices E and A are found as (21) and (22) and lie derivative operator $\mathcal{L}$ is defined as (23), [16].

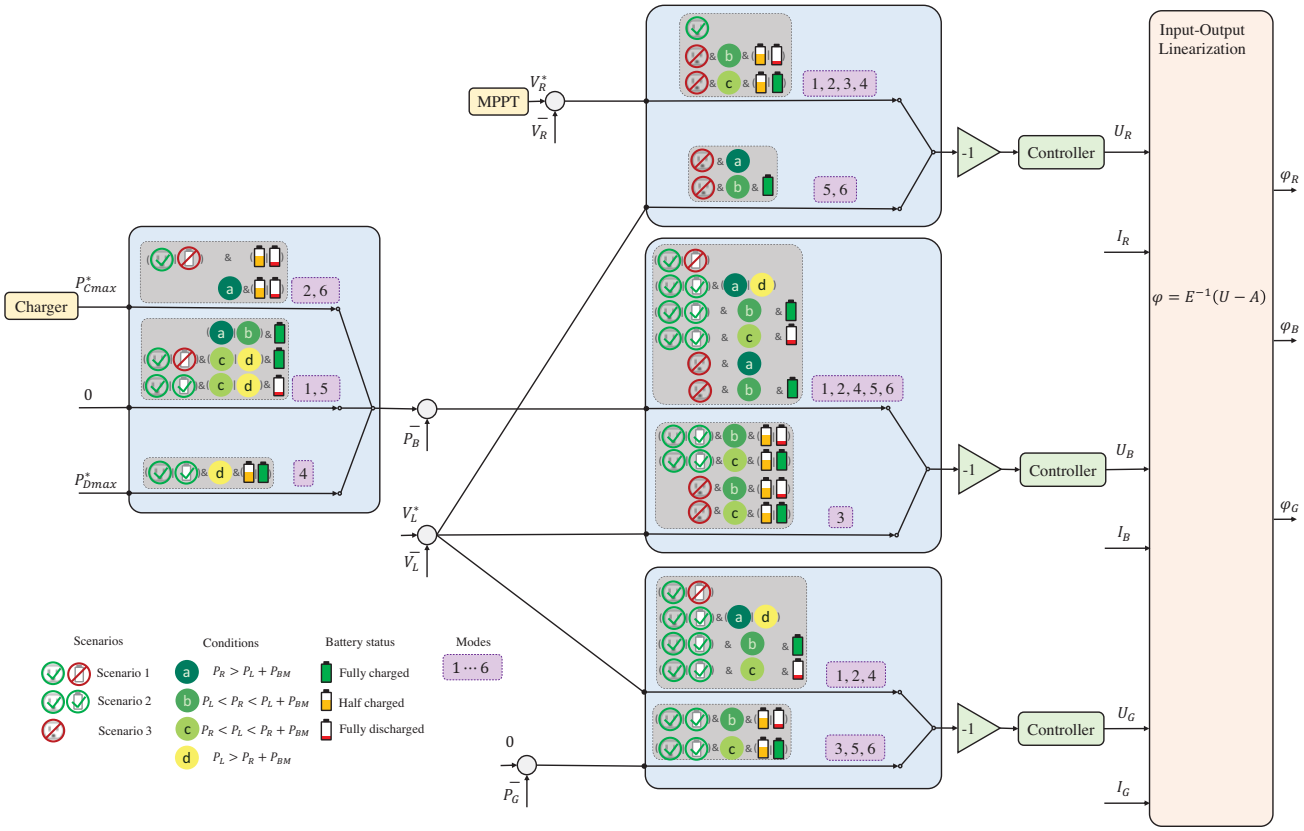

Fig. 7. The suggested control block diagram for MPSST.

$$E = \begin{pmatrix} \mathcal{L}_{g_R} I_R & \mathcal{L}_{g_B} I_R & \mathcal{L}_{g_G} I_R \\ \mathcal{L}_{g_R} I_B & \mathcal{L}_{g_B} I_B & \mathcal{L}_{g_G} I_B \\ \mathcal{L}_{g_R} I_G & \mathcal{L}_{g_B} I_G & \mathcal{L}_{g_G} I_G \end{pmatrix} \tag{21}$$

$$A = \begin{pmatrix} \mathcal{L}_f I_R \\ \mathcal{L}_f I_B \\ \mathcal{L}_f I_G \end{pmatrix} \tag{22}$$

$$\mathcal{L}_g f = (\nabla f) \times g \tag{23}$$

Applying general form of equations (21), (22) to the system equations (20), yields the linearization matrices (25), (26).

$$E = \frac{1}{8L_l} \begin{pmatrix} 3 & -1 & -1 \\ -1 & 3 & -1 \\ -1 & -1 & 3 \end{pmatrix} \tag{24}$$

$$E^{-1} = L_l \begin{pmatrix} 4 & 2 & 2 \\ 2 & 4 & 2 \\ 2 & 2 & 4 \end{pmatrix} \tag{25}$$

$$A = -\frac{V_L}{8L} + \frac{r}{L} \begin{pmatrix} I_R \\ I_B \\ I_G \end{pmatrix} \tag{26}$$

The general form of linearization law is obtained in (27) and the final form of the linearization system of the MPSST is (28).

$$\varphi = E^{-1}(U - A) \tag{27}$$

$$\begin{pmatrix} \varphi_R \\ \varphi_B \\ \varphi_G \end{pmatrix} = E^{-1} \times \begin{pmatrix} U_R - (r/L) I_R + V_L/8L \\ U_B - (r/L) I_B + V_L/8L \\ U_G - (r/L) I_G + V_L/8L \end{pmatrix} \tag{28}$$

V. The Control Scheme

The renewable is operating at the maximum power point tracking when the grid is available or the autonomous operation when there is a path for the power. There are total of 7 modes of operation which are shown in Fig. 6. The block diagram of Fig.7 suggests a coherent way to achieve all of these 7 modes with switches to change from one mode to another. Hysteresis switches are suggested to make a better transition from one mode to another. Since the reference angle on the load port is $\varphi_L = 45°$ the output of other controllers is limited to $0-90°$. The converter with the smallest angle delivers the highest power to the rest. The converter with the highest angle receives the most power. The negative sign before the controller in the block diagram is inserted to compensate for the reverse relation between the phase shift angle and power.

To demonstrate the effectiveness of the proposed control system one of the simulation is presented here which is in scenario 2, battery status of half full and covers all four conditions. The trajectory of the operating point is shown in

Fig. 8. The condition starts with high renewable and low load power to low renewable and high load power condition. Each operating point is numbered 1 to 7. These numbers are shows in the corresponding power on each transformer ports power plot Figs. 9-12.

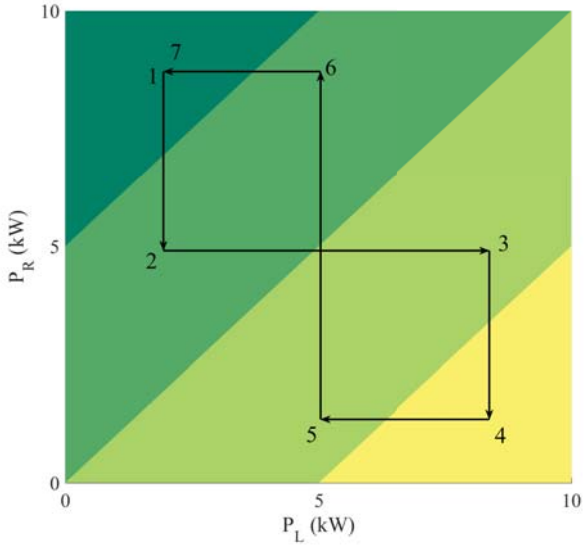

Fig. 8. The trajectory of operating point variation due to the load or renewable power variation.

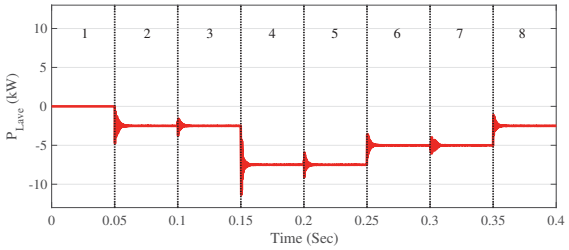

Fig. 9. The power at the load port of the MPSST.

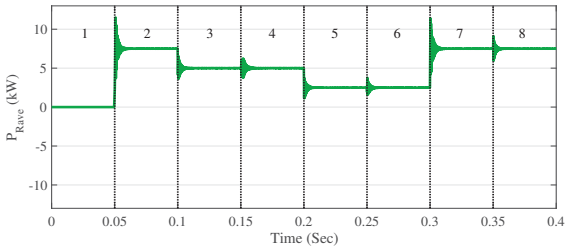

Fig. 10. The power at the renewable port of the MPSST.

VI. Conclusion

In this paper a control strategy for the MPSST is suggested. Three scenarios of operation principle policies and several conditions of renewable and load power, and battery SOC

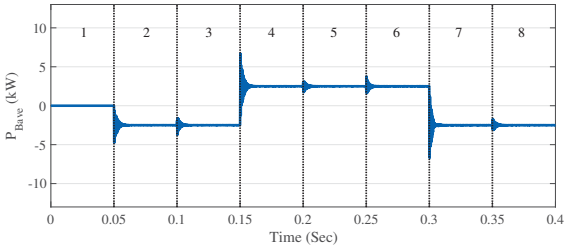

Fig. 11. The power at the battery port of the MPSST.

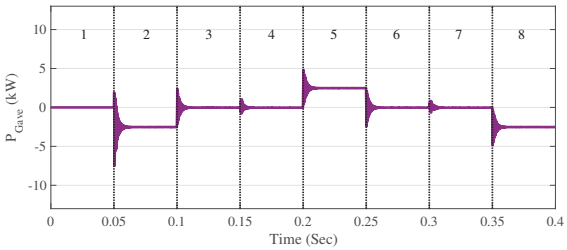

Fig. 12. The power at the grid port of the MPSST.

are considered. Despite various conditions, it is shown that only 7 modes of operation are needed to control the system which leads to 7 control structure. Conditioned switches are implemented to automatically switch between these modes and hysteresis switches are suggested for the transition from one mode to another. Simulation results are presented by several sharp variation of the load and renewable energy source and the power regulation at each port of the transformer is demonstrated.

Acknowledgment

This material is based upon work supported by the National Science Foundation under Grant No. 1650470. Any opinions, findings, and conclusions or recommendations expressed in this material are those of the author(s) and do not necessarily reflect the views of the National Science Foundation.

Dr. Necmi Altin thanks financial support which he received from the Scientific and Technological Research Council of Turkey (TUBITAK) BIDEB-2219 Postdoctoral Research program.

References

[1] Q. Zhu, L. Wang, A. Huang, K. Booth, and L. Zhang, "7.2 kV Single Stage Solid State Transformer Based on Current Fed Series Resonant Converter and 15 kV SiC MOSFETs," *IEEE Transactions on Power Electronics*, pp. 1–1, 2018.

[2] A. C. Nair and B. G. Fernandes, "A Novel Multi-Port Solid State Transformer Enabled Isolated Hybrid Microgrid Architecture," in *IECON 2017 - 43rd Annual Conference of the IEEE Industrial Electronics Society*, Oct 2017, pp. 651–656.

[3] M. Rashidi, A. Bani-Ahmed, and A. Nasiri, "Application of a Multi-Port Solid State Transformer for Volt-VAR Control in Distribution Systems," in *2017 IEEE Power Energy Society General Meeting*, July 2017, pp. 1–4.

[4] S. Ozdemir, S. Balci, N. Altin, and I. Sefa, "Design and Performance Analysis of the Three-Level Isolated DC-DC Converter with the Nanocyrstalline Core Transformer," *International Journal of Hydrogen Energy*, vol. 42, no. 28, pp. 17 801 – 17 812, 2017, special Issue on The 4th European Conference on Renewable Energy Systems (ECRES 2016), 28-31 August 2016, Istanbul, Turkey. [Online]. Available: http://www.sciencedirect.com/science/article/pii/S0360319917307280

[5] V. N. S. R. Jakka, A. Shukla, and G. D. Demetriades, "Dual-Transformer-Based Asymmetrical Triple-Port Active Bridge (DT-ATAB) Isolated DCDC Converter," *IEEE Transactions on Industrial Electronics*, vol. 64, no. 6, pp. 4549–4560, June 2017.

[6] M. Rashidi, A. Nasiri, and R. Cuzner, "Application of Multi-Port Solid State Transformers for Microgrid-Based Distribution Systems," in *2016 IEEE International Conference on Renewable Energy Research and Applications (ICRERA)*, Nov 2016, pp. 605–610.

[7] C. Gu, Z. Zheng, L. Xu, K. Wang, and Y. Li, "Modeling and Control of a Multiport Power Electronic Transformer (PET) for Electric Traction Applications," *IEEE Transactions on Power Electronics*, vol. 31, no. 2, pp. 915–927, Feb 2016.

[8] L. F. Costa, G. Buticchi, and M. Liserre, "Quadruple Active Bridge DC-DC converter as the basic cell of a modular Smart Transformer," in *2016 IEEE Applied Power Electronics Conference and Exposition (APEC)*, March 2016, pp. 2449–2456.

[9] M. Phattanasak, R. Gavagsaz-Ghoachani, J. Martin, B. Nahid-Mobarakeh, S. Pierfederici, and B. Davat, "Control of a Hybrid Energy Source Comprising a Fuel Cell and Two Storage Devices Using Isolated Three-Port Bidirectional DCDC Converters," *IEEE Transactions on Industry Applications*, vol. 51, no. 1, pp. 491–497, Jan 2015.

[10] L. F. Costa, G. Buticchi, and M. Liserre, "Quad-Active-Bridge as Cross-Link for Medium Voltage Modular Inverters," in *2015 IEEE Energy Conversion Congress and Exposition (ECCE)*, Sept 2015, pp. 645–652.

[11] S. Roy, A. De, and S. Bhattacharya, "Multi-Port Solid State Transformer for Inter-Grid Power Flow Control," in *2014 International Power Electronics Conference (IPEC-Hiroshima 2014 - ECCE ASIA)*, May 2014, pp. 3286–3291.

[12] S. Falcones, R. Ayyanar, and X. Mao, "A DC x2013;DC Multiport-Converter-Based Solid-State Transformer Integrating Distributed Generation and Storage," *IEEE Transactions on Power Electronics*, vol. 28, no. 5, pp. 2192–2203, May 2013.

[13] X. She, A. Q. Huang, and R. Burgos, "Review of Solid-State Transformer Technologies and Their Application in Power Distribution Systems," *IEEE Journal of Emerging and Selected Topics in Power Electronics*, vol. 1, no. 3, pp. 186–198, Sept 2013.

[14] W. McMurray, "The Thyristor Electronic Transformer: a Power Converter Using a High-Frequency Link," *IEEE Transactions on Industry and General Applications*, vol. IGA-7, no. 4, pp. 451–457, July 1971.

[15] B. Zhao, Q. Song, W. Liu, and Y. Sun, "Overview of Dual-Active-Bridge Isolated Bidirectional DC x2013;DC Converter for High-Frequency-Link Power-Conversion System," *IEEE Transactions on Power Electronics*, vol. 29, no. 8, pp. 4091–4106, Aug 2014.

[16] M. Khayamy, O. Ojo, and E. Sota, "Non-Linear Controller Approach for an Autonomous Battery-Assisted Photovoltaic System Feeding an AC Load with a Non-Linear Component," *Renewable Power Generation, IET*, vol. 8, no. 8, pp. 838–848, 2014.